



## LOWER BOUNDS AND SATURATION EFFECTS OF DYNAMIC FRACTURE TOUGHNESS IN THE BRITTLE-TO-DUCTILE TRANSITION REGIME OF FERRITIC STEELS

Hans-Jakob Schindler<sup>1</sup> and Dietmar Kalkhof<sup>2</sup>

<sup>1</sup> Mat-Tec AG, Winterthur, Switzerland (schindler@mat-tec.ch)

<sup>2</sup> Swiss Federal Nuclear Safety Inspectorate (ENSI), Brugg, Switzerland

### ABSTRACT

In the ductile-to-brittle transition regime fracture toughness of ferritic steels is affected by an inherent scatter. In the present paper lower bounds of initiation toughness under elevated loading rates and its relation to the lower bound of arrest toughness  $K_{Ia}(T)$  are considered theoretically and experimentally. As a representative test material RPV-steel 22NiMoCr37 was used. Lower-bounds of fracture toughness at elevated loading rates are derived by extending a semi-empirical method suggested by the authors for quasi-static loading. By the general Zener-Holomon-relation the rate-induced shift of the lower bounds can be extrapolated to higher loading rates. In this way it was found that the lower-bound of initiation toughness  $K_{Id}(T)$  coincides with  $K_{Ia}(T)$  at a loading rate of about  $1.7 \cdot 10^6$  MPa·m<sup>0.5</sup>/s, although the latter corresponds to a much higher loading rate. Thus, the rate-effect on fracture toughness seems to saturate at about this loading rate. Consequently, the lower bound  $K_{Ia}(T)$  represents a lower bound for initiation toughness at maximum impact loading rates. In reverse, this finding enables the reference temperature of arrest toughness according to ASTM E1221,  $T_{K_{Ia}}$ , to be estimated from  $T_{0,x}$  determined according to ASTM E1921 by impact tests.  $T_{K_{Ia}}$  and  $T_{0,x}$  values for high loading rates determined by Boehme et al. (2013) and Mayer (2012) are in good agreement with the theoretical predictions. There are indications that the procedure of ASTM E1921 to determine  $T_0$  should be modified when applied to elevated or high loading rates.

### INTRODUCTION

In the ductile-to-brittle transition (DBT) regime fracture toughness of ferritic steels is affected by an inherent scatter, which requires statistical evaluation of test data. A well-known method is the procedure according to ASTM E1921 that is based on the master-curve (MC) suggested by Wallin (1992). The corresponding reference temperature  $T_0$ , is evaluated based on Weibull statistics. However, as shown by Heerens et al (2002), Weibull statistics fails to describe the scatter for low cumulative failure probabilities ( $p_f$ ). Though suitable to determine  $T_0$  from a set of test data, the procedure of ASTM E1921 is hardly capable to predict fracture toughness at  $p_f < 2.5\%$ , which is the most relevant range of failure probabilities for engineering purposes. Furthermore, the 3-parameter Weibull statistics used in ASTM E1921 does not exhibit the correct asymptotic behavior for the application to large structural components. Actually, as discussed by Anderson and Rosel (2010) and Schindler et al. (2008) a physical lower bound is expected to exist that depends at least on the temperature and the yield stress. These physical aspects are not adequately accounted for in the MC-approach, which is probably the main reason why the corresponding predictions of  $K_{Jc}$  at low failure cumulative probabilities often fail to be realistic. Further drawbacks of MC-based tolerance bounds are their limitation to  $T_0 - 50^\circ\text{C} < T < T_0 + 50^\circ\text{C}$ , which means that a substantial, practically relevant part of the DBT-range is not covered, and the uncertainty of  $T_0$  due to several influencing factors and biases (Kalkhof and Schindler (2012)).

For these reasons, to show structural safety of a component in the DBT-regime analytically it is usually preferable to consider conservative lower bounds of plane strain fracture toughness. For RPV-steels, which are medium-strength structural steels, an empirically well-founded lower-bound is provided by ASME (2004) to be

$$K_{Ic(ASME)}(T) = 36.5 + 22.8 \cdot \exp[0.036 \cdot (T - T_0 - 19.4K)] \quad (1)$$

Schindler and Kalkhof (2010, 2013) suggest a model which enables lower bounds to be derived from limited numbers of  $K_{Jc}$ -data measured on smaller specimens. They obtained a lower bound that agreed quite well with eq. (1). A brief summary of the approach is given below. This independent semi-analytical derivation of eq. (1) confirms this empirical relation and leads to the conclusion that it is applicable not only to the RPV-steels considered in ASME (2004), but to all steels that are covered by ASTM E1921, i.e. ferritic/bainitic steels up to a yield stress of 825 MPa. Applied to components that are thinner than the thickness required for plane strain behavior, eq. (1) tends to be over-conservative, which is the main drawback of (1). Corresponding remedy is possible by the model suggested by Schindler and Kalkhof (2010, 2013) that enable size-corrected lower bounds of  $K_{Jc}$  to be obtained from.

In the BDT-range fracture toughness is well known to be sensitive to the loading rate. In cases of elevated loading rates, (1) tends to be non-conservative, unless  $T_0$  is determined at a correspondingly increased loading rate.

$$K_{Ia(ASME)}(T) = 29.4 + 13.697 \cdot \exp[0.0261 \cdot (T - T_0 - 19.4K)], \quad (2)$$

which is provided in ASTM (2004) as a lower bound for crack arrest toughness, might be considered as a more conservative lower bound for toughness at higher loading rates. However, it is not clear whether or not (2) is conservative in any case of dynamic loading, and how to deal with medium loading rates. In the present paper the effect of the loading rate on  $T_0$  and its relation to lower bounds of fracture toughness and to crack arrest toughness is investigated.

## IMPACT LOADING VS. CRACK ARREST

Because of the autonomy of the fracture process zone that is presumed in engineering fracture mechanics the mechanisms that proceed in the fracture process zone are governed by the stress intensity factor  $K_I$  and its rate  $\dot{K}_I$ . Thus, there must be similarities between cleavage initiation, fast crack propagation and crack arrest. Crack initiation requires a stress peak that exceeds the cleavage stress, a sufficient amount of elastic energy stored in the critical volume around the stress-peak, and the presence of a weak or brittle particle in the vicinity of the stress-peak to trigger the event. The higher the energy density – which is increasing with increasing yield stress in case of increased loading rates - the smaller the critical volume and the closer the stress-peak to the crack tip. With increasing loading rate the fracture process zone shrinks closer and closer to the crack front due to the local increase of dynamic yield strength. Correspondingly, there is a limiting loading rate where the fracture origin is so close to the crack-front, that initiation no longer requires a weak particle to be triggered, but spreads out from micro-structural features at the crack front.

Cleavage crack propagation is an unstable process, since  $K_I$  required to initiate cleavage is higher than the one to maintain dynamic crack propagation. Moreover, there is a positive feed-back from the relation between local dynamic yield-stress and crack-speed as follows: An increasing crack extension rate increases the local strain rate and correspondingly the local yield stress, leading to increasing brittleness. Thus, a cleavage crack tends to a certain limiting speed that is bound by the energy flow to the crack-tip (Freund 1972). Correspondingly, the limiting speed is in the order of half of the Raleigh-wave-

speed, i.e. about 1000 m/s. If the energy flux is no longer sufficient to maintain dynamic crack propagation, the crack stops immediately. Thus, a cleavage crack either propagates rapidly, or it stops, there is not much in between. This means that crack arrest toughness represents the  $K_I$  required for rapid crack-propagation. Crack arrest may be accompanied by a “ringing-down” as shown by Kalthoff et al. (1977), which can cause a stop-and-go process prior to arrest. Nevertheless, the arrest toughness still corresponds to the toughness at high crack extension rates.

For dimensional reasons a representative strain rate in the fracture process zone due to rapid loading can be defined as

$$\dot{\epsilon}_L \approx \frac{\dot{\delta}}{\delta_c} = 2 \cdot \frac{\dot{K}_I}{K_{Id}} \quad (3)$$

where  $\delta_c$  and  $\dot{\delta}$  denote the crack-tip opening displacement (CTOD) and its rate, respectively.  $K_{Id}$  is the dynamic fracture toughness. A Dugdale-type strip yield model can be used to estimate  $\delta$  and  $\dot{\delta}$  for a propagating crack. This leads to

$$\dot{\epsilon}_L \approx \frac{\dot{\delta}}{\delta_c} \approx \frac{\dot{a}}{r_c} \approx \frac{8}{\pi} \cdot \frac{m^2 \cdot R_{pd}^2 \cdot \dot{a}}{K_{Id}^2(\dot{a})} \quad (4)$$

where  $r_c$  denotes the length of the strip-shaped yield zone and  $R_{pd}$  the dynamic yield stress. By equalizing (3) and (4) one obtains the equivalent loading rate in terms of  $\dot{K}_I$  that is associated with a crack extension rate  $\dot{a}$  as follows:

$$\dot{K}_{Ieq} = \frac{4}{\pi} \cdot \frac{m^2 \cdot R_{pd}^2 \cdot \dot{a}}{K_{Id}} \quad (5)$$

Thus, inserting  $\dot{a}=1000$  m/s,  $m=2$  and  $R_{pd}=1000$ MPa and  $K_{Id}=50$  MPa·m<sup>0.5</sup> as typical values for medium strength steel (5) delivers

$$\dot{K}_{Ieq} \cong 1.0 \cdot 10^8 \text{ MPa} \cdot \text{m}^{0.5} / \text{s} \quad (6)$$

Of course this is only a rough estimate but sufficient to show that the loading rate at a running cleavage crack is higher by at least one order of magnitude than loading rates due to high-rate tests such as drop-weight or Hopkinson bar. This means that crack arrest toughness corresponds to a loading rate that can hardly be achieved by impact loading (disregarding ballistics), so crack arrest toughness could be a lower bound of impact toughness indeed. However, the relation between arrest-toughness and impact-toughness should be clarified. Regarding the high loading rate that is associated with crack arrest, the question is how arrest-toughness can be used to estimate initiation-toughness at impact loading rates.

Concerning the statistical behavior, a fundamental difference is expected to exist between initiation toughness  $K_{Ic}$ , and arrest toughness  $K_{Ia}$ . Unlike the former, crack arrest does not depend on the stochastic presence of a single weak particle in the critical zone. In fact, a particle that is able to trigger unstable cleavage is not able to stop a running crack. As discussed in Schindler and Kalkhof (2013) and briefly below, this behavior is related to lower bounds of initiation toughness, which reflects the crack load required to initiate cleavage in case of a sufficient number of possible cleavage origins. This similarity between arrest toughness and lower bounds of initiation toughness implies that comparisons

between them should be made on the basis of lower bound curves of initiation toughness. Such lower bounds at elevated loading rates are considered in the next section.

## LOWER BOUNDS OF FRACTURE TOUGHNESS AT INCREASED LOADING RATES

According to Schindler and Kalkhof (2013) it is likely that a saturation of the statistical weakest-link-effect occurs at a certain thickness  $B_{sat}$ . The latter was found to be close to the thickness required by ASTM E399 for plane-strain fracture toughness, i.e.

$$B_{sat} \approx B_{p\epsilon} = 2.5 \cdot \left( \frac{K_{Jc}}{R_p} \right)^2, \quad (7)$$

where  $R_p$  denotes the yield stress. This confirms the hypothesis of Merkle et al. (2002) (see also McCabe and Merkle (1997)), who postulated a saturation of the thickness-effect according to Weibull-statistics at a thickness  $B=B_{p\epsilon}$ . This assumption enabled them to calculate the plane strain fracture toughness  $K_{Ic}$  corresponding to a measured  $K_{Jc}$  value, as sketched in Fig. 1. On a similar basis Schindler and Kalkhof (2010, 2013) derived the following simple formula to estimate the equivalent  $K_{Ic}$ -value from  $K_{Jc}$  measured by a specimen of the thickness  $B_T$ :

$$K_{Ic}(p_f) = 0.858 \cdot R_p^{1/3} \cdot B_T^{1/6} \cdot K_{Jc}^{2/3}(B_T, p_f) \quad \text{for } B_T < B_{p\epsilon} \quad (8a)$$

$$K_{Ic}(p_f) = K_{Jc}(B_T, p_f) \quad \text{for } B_T > B_{p\epsilon} \quad (8b)$$

Note that  $K_{Ic}$  as obtained by (8) is associated with the same failure probability as the original  $K_{Jc}$ . Correspondingly, if (8) is applied to a lower envelope of a sufficient number of tests data, it is expected to deliver a lower bound of  $K_{Ic}(T)$ . In fact, by this procedure Schindler and Kalkhof (2013) obtained a curve very close to eq. (1) based only on relatively few test data from specimens with thicknesses  $B_T < B_{p\epsilon}$ . From this independent semi-analytical determination of eq. (1) one can conclude that the latter is applicable not only to the RPV-steels that it is originally empirically derived from, but, corresponding to the application range of ASTM E1921, to all ferritic/bainitic steels with  $R_p < 825$  MPa.

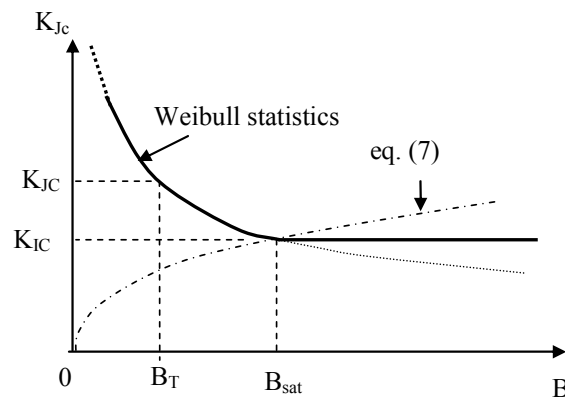


Fig. 1: Dependence of  $K_{Jc}$  on the thickness  $B$

The derivation of (8) is not restricted to quasi-static loading, so it can be applied to experimental  $K_{Jc}$ -data from tests under elevated loading rates as well, which are denoted in the following as  $K_{Jd}$ . In this

case, the yield stress should be chosen at the corresponding local strain rate. However,  $R_p$  appears in (8) only by the power of 1/3, so a rough estimate of the rate effect on  $R_p$  is sufficient.

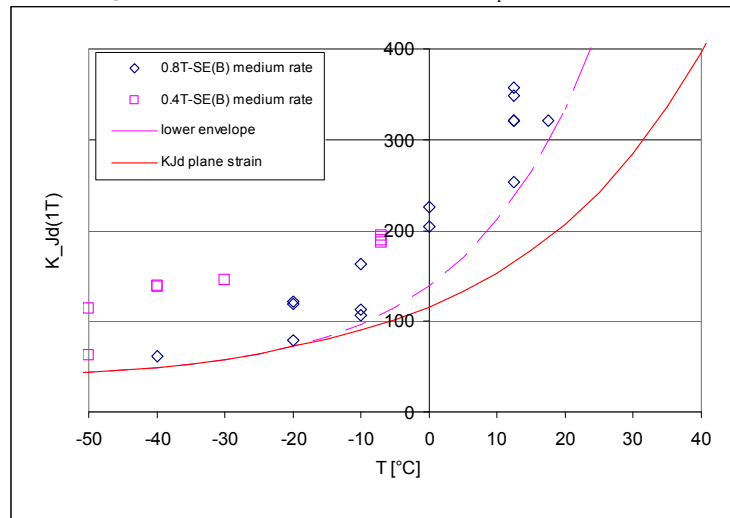


Fig.2: Experimental  $K_{Jd}$ -data at medium loading rate normalized to a thickness of 1T (24.5 mm)

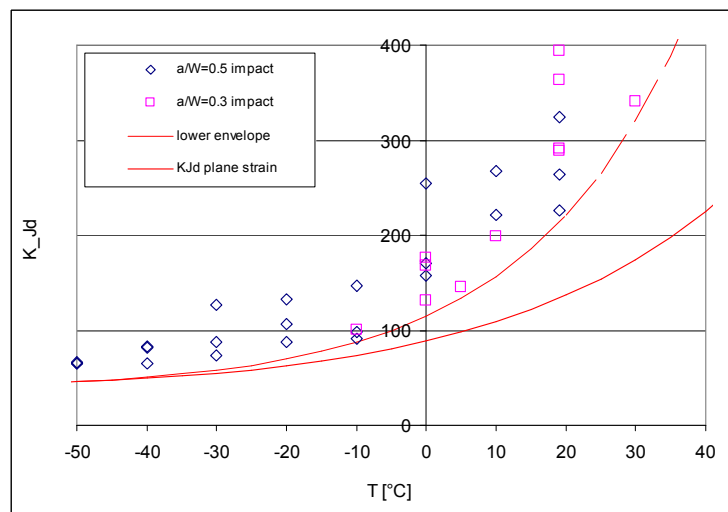


Fig. 3:  $K_{Jd}$ -data obtained from pre-cracked-Charpy specimens at an impact rate of 2m/s.

Fig. 2 shows  $K_{Jd}$ -values obtained from SEB-specimens of the RPV-steel 22NiMoCr3 at a loading rate of about  $\dot{K}_I = 5700 \text{ MPa}\sqrt{\text{m/s}}$  (thickness  $B_T = 20 \text{ mm}$ ) and  $7000 \text{ MPa}\sqrt{\text{m/s}}$  (thickness  $B_T = 10 \text{ mm}$ ), normalized according to ASTM E1921 to the standard thickness  $B_T = 25.4 \text{ mm}$  (see Viehrig et al 2010) for experimental details). Following the procedure described in Schindler and Kalkhof (2013) for quasi-static data, the dashed line in Fig. 2 was drawn as an estimated lower envelope of the experimental data. By transforming this curve by eq. (8) a the full line in Fig. 2 is obtained, that is expected to represent a lower bound of  $K_{Jd}(T)$ . In Fig. 3  $K_{Jd}$ -data measured on pre-cracked Charpy specimens ( $B_T = 10 \text{ mm}$ ) with crack-depths  $a_0/W = 0.5$  and  $a_0/W = 0.3$  at a impact rates of  $\dot{K}_I = 150000 \text{ MPa}\sqrt{\text{m/s}}$  and  $300000 \text{ MPa}\sqrt{\text{m/s}}$ , respectively, are treated in the same way, which leads with eq. (8) to the lower bound  $K_{Jd}(T)$  that is shown in Fig. 3.

## SATURATION OF RATE-INDUCED EMBRITTLEMENT

Fig. 4 shows the lower bounds determined in Figs. 2 and 3 as well as the one determined analogously for quasi-static loading in Schindler and Kalkhof (2013), in comparison with the lower bounds given by eqs. (1) and (2) for the reference temperature of the considered steel,  $T_0 = -71^\circ\text{C}$ . The curve for impact loading rate is relatively close to (2), so it is expected to coincide with (2) if the loading rate would be further increased by a certain amount. In order to estimate the corresponding loading rate we introduce the reference temperatures  $T_{100LB}$  as the temperatures at which the rate-dependent lower bounds equals  $100 \text{ MPa}\cdot\text{m}^{0.5}$  (see Fig. 4). Like any reference temperature that depends on the yield strength,  $T_{100LB}$  is related to the loading rate by

$$T_{100LB} [K] \cdot \ln \frac{\dot{K}_0}{\dot{K}_I} = \text{const} \quad (9)$$

which follows from the hypothesis of thermal activation of plastic flow (“Holomons law”, see Priest (1977), Schindler and Morf (1992)). In (9)  $\dot{K}_0$  represents a reference value of  $\dot{K}_I$ . Fitting (9) to the experimental values of  $T_{100LBx}$  and  $T_{100LBs}$  that are taken from Fig. 4, the relation

$$T_{100LBx} [^\circ\text{C}] = \frac{2499}{9.98 - \log \dot{K}_I} - 273 \quad (10)$$

is obtained. Eq. (10) can be used to interpolate or, to some extent, even extrapolate experimental  $T_{100LBx}$  values. Thus, it can be used to determine  $\dot{K}_I$  for which  $T_{100LBx}$  equals  $T_{100LBa}$  where the latter is introduced in Fig. 4 as the temperature at which  $K_{Ia(ASME)}$  (eq. (2)) equals  $100 \text{ MPa}\cdot\text{m}^{0.5}$ , i.e.  $T_{100LBa} \approx 11^\circ\text{C}$ . The corresponding loading rate, denoted as  $\dot{K}_{Isat}$ , is found from (10) to be

$$\dot{K}_{Isat} = 1.70 \cdot 10^6 \text{ MPa}\cdot\text{m}^{0.5}/\text{s} \quad (11)$$

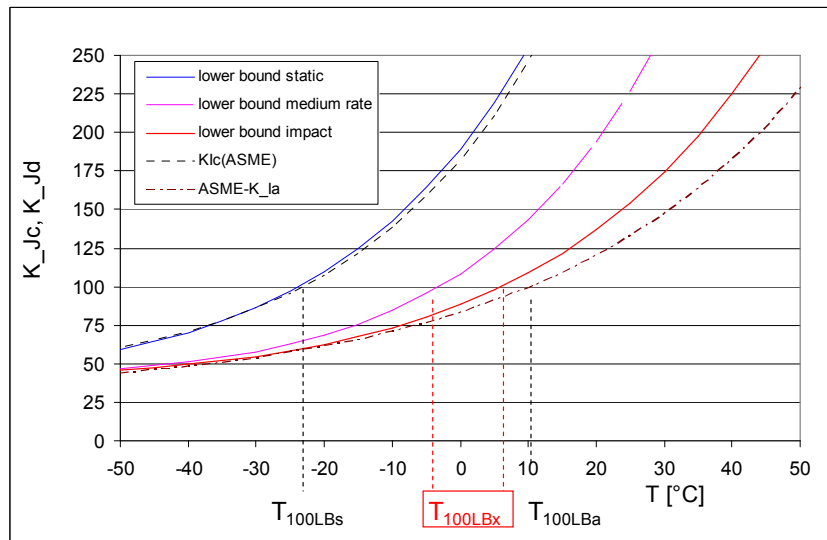


Fig.4: Lower bounds at elevated loading rates in comparison with quasi-static lower bound and eqs. (1) and (2), with definition of reference temperatures  $T_{100LBx}$ .

According to eq. (6) the loading rate of a propagating or arresting crack is at least one order of magnitude higher than the loading rate given in (11), but both are associated with essentially the same lower bound. This implies a saturation of the rate-induced embrittlement at  $\dot{K}_I = \dot{K}_{I, \text{sat}}$ , which means that no further embrittlement occurs in the range  $\dot{K}_I > \dot{K}_{I, \text{sat}}$ .

The saturation of the effect of the loading rate on  $K_{I,d}$  can be explained physically as follows: As discussed above, increasing the loading rate causes the stress-peak appears closer to the crack-tip due to the reduced CTOD, so the cleavage origin at high rates is located closer to the crack tip than at lower rates. If the distance of the stress-peak from the crack-tip is only in the order of the micro-structural dimensions, the fracture process zone is part of the crack-front. In this state, initiation of cleavage no longer needs to be triggered by a weak particle ahead of the crack-tip, and the physical process of crack-initiation becomes similar to the one of crack propagation. This model would also explain the changing statistical distribution at higher loading rates that is found by Boehme et al. (2013).

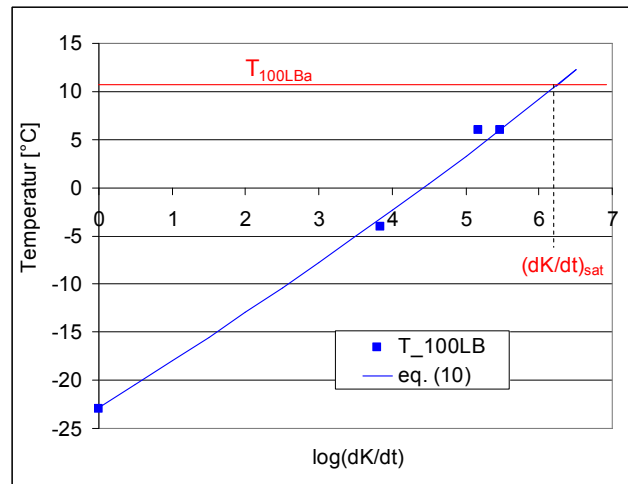


Fig. 5: Reference-temperature  $T_{100LB}$  for lower bounds of  $K_{I,d}$  as a function of the loading rate for the RPV-steel 22NiMoCr3.

## EFFECT OF LOADING RATE ON REFERENCE TEMPERATURE

Fracture toughness in the DBT-range can be characterized by  $T_0$ . In case of elevated loading rates it is denoted as  $T_{0,x}$ , where the index  $x$  is meant to indicate the loading rate in terms of  $\log \dot{K}_I$ . By fitting Holomon's law (see eq. (9)) to the experimental data of Viehrig et al. (2010) and combining it with the temperature shift suggested by Rolfe and Barsom (1977), Schindler and Kalkhof (2013b) obtained the following simple formula to estimate  $T_{0,x}$  for ferritic and bainitic steels with yield strengths  $R_{p0.2} < 825$  MPa as a function of the loading rate<sup>1</sup>:

$$T_{0,x} [^{\circ}\text{C}] = \frac{(T_0 + 273) \cdot \Gamma}{\Gamma - \log \dot{K}_I} - 273, \quad (12a)$$

$$\text{where } \Gamma = \frac{T_0 - 0.12 \cdot R_p + 392}{21.10 - 0.0213 \cdot R_p} \quad (12b)$$

<sup>1</sup> A similar relation is provided in ASTM E1921, but comparisons with experimental data made by the authors indicate that eq. (12b) in general performs better.

In (12)  $T_0$  has to be inserted in °C,  $R_p$  (yield stress at room temperature) in MPa and  $\dot{K}_I$  in  $\text{MPa}\cdot\text{m}^{0.5}/\text{s}$ . Applied to the present test material ( $T_0=-71^\circ\text{C}$ ,  $R_{p0.2}=424\text{MPa}$ ) the dotted line in Fig. 6 is obtained from (12). The saturation of the rate-effect on initiation toughness at  $\dot{K}_I = \dot{K}_{I\text{sat}}$  implies that the rate-induced shift  $T_0 - T_{0,x}$  quantified by (12) saturates at the loading rate given by (11), too. This means that (12) is valid only for  $\dot{K}_I < \dot{K}_{I\text{sat}}$  and that  $T_{0,x}$  stays constant for  $\dot{K}_I > \dot{K}_{I\text{sat}}$  at a limiting value  $T_{0\text{sat}}$ . The corresponding prediction of  $T_{0,x}$  as a function of  $\dot{K}_I$  is shown as the dotted red line in Fig. 6. With  $\dot{K}_{I\text{sat}}$  from (11) inserted in (12)  $T_{0\text{sat}}$  is obtained to be

$$T_{0,\text{sat}} = T_{0,6} = 6.8^\circ\text{C} \quad (13)$$

The rationale provided in the previous section for a saturation of the rate effect at  $\dot{K}_I = \dot{K}_{I\text{sat}}$  implies that  $T_{0,\text{sat}}$  represents the reference temperature of arrest toughness,  $T_{\text{Kla}}$  according to ASTM E 1221. By inserting  $\dot{K}_I = \dot{K}_{I\text{sat}}$  from (11) in (12) the following simple formula to estimate  $T_{\text{Kla}}$  is obtained:

$$T_{\text{Kla}} \approx T_{0,\text{sat}} [^\circ\text{C}] \approx \frac{T_0 + 273}{1 - \frac{131.4 - 0.133 \cdot R_p}{T_0 + 392 - 0.12 \cdot R_p}} - 273 \quad (14)$$

Since (11) is expected to be not much strength-dependent, (14) is expected to hold not only for the RPV-steels in question, but as an approximation to a wider range of ferritic or bainitic steels with  $R_p < 825$  MPa.

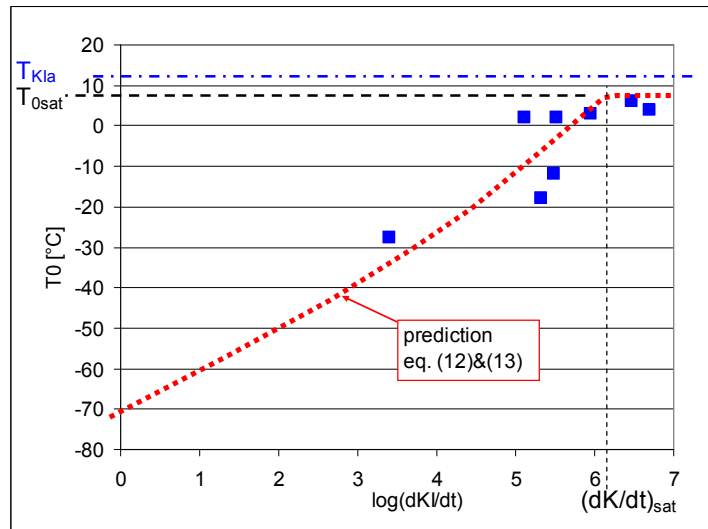


Figure 6: Experimental  $T_{0,x}$ -data from Boehme et al. (2012) evaluated with  $p=0.3$  and  $T_{\text{Kla}}$  from Mayer (2012) compared with predictions obtained from eqs. (11) – (14)

## COMPARISON WITH EXPERIMENTAL DATA

Boehme et al. (2012, 2013) and Mayer (2012) investigated the fracture behavior of RPV-steels in the DBT-range under very high loading rates. As a test material they used the same RPV-steel as in the present study. The test program included a number of high-rate tests by impact bending and Hopkinson

bar tests as well as crack arrest tests according to ASTM E 1221.  $T_{0,x}$  evaluated according to E1921 exhibited significant inconsistencies between specimen sizes and shapes. Some of the  $T_{0,x}$  even exceeded  $T_{K1a}$ , which is unlikely according to the considerations above. Possible reasons for these inconsistencies were identified and discussed by Boehme et al. (2013), including a deviation of the  $K_{Jd}$ -data from the Weibull-distribution and the distortion of the shape of the MC at higher loading rates. The latter corresponds to an effect that has been observed by Schindler and Kalkhof (2013b) and Kalkhof and Schindler (2012): They found that the coefficient  $p=0.019$  in the exponent of the MC according to ASTM E1921 tends to increase with increasing loading rates, what makes  $T_{0,x}$  dependent on the test temperature.

In fact, if the data from Boehme et al. (2013) are evaluated by assuming the corresponding coefficient in ASTM E1921 to be  $p=0.3$  instead of the standard value 0.019, the span of variation of the obtained  $T_{0,x}$  shrinks significantly and their maximum is reduced to a value below  $T_{K1a}$ . The correspondingly modified  $T_{0,x}$  data are shown in Fig. 6. The agreement with the prediction is remarkably good: In fact, the experimental  $T_{0,x}$  exhibit the predicted kink of the trend-line at  $\dot{K}_I = \dot{K}_{I_{sat}}$ , and a saturation effect in the range  $\dot{K}_I > \dot{K}_{I_{sat}}$  can be recognized. Furthermore,  $T_{K1a}$  as predicted by (14) is in good agreement with the measured  $T_{K1a}$ . These data also confirm that  $T_{K1a}$  represents an upper limit of  $T_{0,x}$ .

## DISCUSSION AND CONCLUSIONS

The good agreement of the predicted  $T_{0,x}$ -values with the ones independently measured by Boehme et al. (2013) confirms the theoretical models and assumptions behind the predictions. There are theoretical and experimental indications that the rate-induced embrittlement, which manifests in a rate-dependent shift of  $T_{0,x}$  and the lower bound of  $K_{Jd}(T)$  to higher temperatures, reaches a saturation at about  $\dot{K}_I = 1.7 \cdot 10^6 \text{ MPa} \cdot \text{m}^{0.5}/\text{s}$  for the considered steel (eq. (11)). Moreover, it is shown that impact toughness and arrest toughness are closely related to each other. The latter represents fracture toughness at a very high loading rate that can hardly be achieved by impacts or structural waves, apart from ballistic loading. Therefore, it can be assumed that arrest toughness represents a lower bound of impact toughness. Lower bounds of dynamic fracture toughness appear to be better suited for practical applications. In the present paper a method to derive rate-dependent lower bounds of  $K_{Jd}$  from experimental  $K_{Jd}$ -data is presented. As far as numerical values are given, these findings apply to the RPV-steel considered here. However, most of them are expected to be extendable, at least as approximations, to other types of structural steels.

There are indications that fracture toughness at high loading rates and crack arrest does not follow the same statistical pattern as quasi-static fracture toughness, which are supported by recent findings of Boehme et al (2013). Schindler and Kalkhof (2013b) observed a rate-dependent distortion of the MC even at relatively low rates. From the present investigation it can be seen that eq. (1) is not applicable to  $T_{0,x}$  at higher rates, since this would result in curves that deviate significantly from the dynamic lower bounds shown in Fig. 4, which also can be an indication for a change in statistical distribution or to the rate-dependent distortion of the MC. For these reasons there are severe doubts or at least questions concerning the applicability of ASTM E1921 to evaluate  $T_{0,x}$  at higher loading rates. Even more questionable is the prediction of fracture toughness from  $T_{0,x}$  by the tolerance bounds given in E1921 in the range of low failure probabilities. Questions like these need to be further clarified.

## REFERENCES

- Anderson T.L., Rose B.D. (2010), "A Modified Weibull Stress Model for Cleavage Fracture that Incorporates Threshold Toughness", Proceedings of 12th Int. Conf on Fracture, Ottawa, 2010

- ASME (2004), Boiler and Pressure Vessel Code, Section XI, Division 1, NB 2331, American Society of Mechanical Engineers, New York, 1999 American Society of Mechanical Engineers, New York.  
See also: ASME Code Case N-629, Section XI, Division 1,
- Böhme, W., Reichert, T. and Mayer U., (2013), “Assessment of Dynamic Fracture Toughness Values  $K_{Ic}$  and Reference Temperatures  $T_{0,x}$  determined for a German RPV steel at elevated loading rates according to ASTM E1921”, to be presented at SMiRT 22, San Francisco, August 2013
- Böhme, W., Mayer, U., Reichert, T. (2012), “Verification and further development of assessment methods for dynamic crack initiation and crack arrest”, IWM-Freiburg, Project No. 150 1368, Report No. 665/2012, 2012
- Freund, LB (1972), “Crack propagation in an elastic solid subjected to general loading”, Part I and II, *J Mechanics and Physics of solids*, 20, 129-152
- Heerens J., Pfuff M., Hellmann D., Zerbst U., “The lower bound toughness procedure applied to the Euro fracture toughness dataset”, *Engineering Fracture Mechanics* 69 (2002) 483–495
- Kalkhof, D., and Schindler, H.J. (2012), “Uncertainties in  $T_0$  and Corresponding Safety Margins in Lower Bounds of  $K_{Ic}$  in the Ductile-to-Brittle Transition Regime of Ferritic Steels”, Proc. of 19th Europ. Conf. on Fracture, Paper ID 257, 25.-31.08.2012, Kazan, RU
- Kalthoff, J.F., Beinart, J, Winkler, S., “Measurement of dynamic stress intensity factor for fast running and arresting cracks”, ASTM STP 627, ASTM, Philadelphia, PA, 161-176
- Mayer, U. (2012), “Determination of dynamic fracture toughness at high loading rates”, Proceedings of the ASME 2012 International Mechanical Engineering Congress & Exposition (IMECE2012), November 2012, Houston, Texas
- McCabe, D.E., and Merkle J.G. (1997), “Estimation of Lower-Bound  $K_{Ic}$  on Pressure Vessel Steels from Invalid Data”, in: ASTM STP 1321, American Soc. For Testing and Materials, West Conshohocken, Pa., 198-213
- Merkle, J.G., Sokolov, M.A., Nanstad, R.K., Mc Cabe, D.E. (2002), “Statistical representation of valid  $K_{Ic}$  Data for irradiated RPV-Steels”, ORNL/NRC/LTR-01/08, Oak Ridge National Laboratory, USA
- Priest, A.H. (1977), “Influence of Strain Rate and Temperature on the fracture and Tensile Properties of Several Metallic Materials”, *Dynamic Fracture Toughness*, The Welding Institute, Cambridge, UK,
- Rolfe, T.H., Barsom, J.M. (1977), “Fracture and fatigue control in structures: Applications of fracture mechanics”, Prentice – Hall.
- Schindler, H.J., and Morf, U. (1992), “Toughness testing and assessment of welds”, Proc. Int. Conf. on Engineering Design in Welded Structures, Madrid, Spain 205-212
- Schindler, H.J., Kalkhof, D., Tipping, Ph. (2008), “Determination of Transferable Lower-Bound Fracture Toughness from Small Specimens”, *J. ASTM International*, Vol. 5, No. 8
- Schindler, H.J., and Kalkhof, D. (2010), “Lower-bound fracture toughness in the transition regime from small specimen data”, *DVM Bericht* 242, S. 217-226 (in German)
- Schindler, H.J., and Kalkhof, D. (2013), “Thickness-dependent lower bounds of fracture toughness of ferritic steels in the ductile-to-brittle transition regime”, 13th International Conference on Fracture, June 16–21, 2013, Beijing, China
- Schindler, H.J. and Kalkhof, D. (2013b), “A closer look at effects of the loading rate on fracture toughness in the ductile-to-brittle transition regime of ferritic steels”, submitted for publication to *J. Testing and Evaluation*.
- Viehrig H.W., Schindler H.J., Kalkhof, D. (2010), “Effects of Test Parameters on the Master Curve Reference Temperature”, 18th Europ. Conf. on Fracture (ECF 18), Dresden, 2010
- Wallin, K. (1992) “Recommendation for Application of Fracture Toughness Data for Structural Integrity Analysis,” Proc. CSNI/IAEA Specialists' Meeting, Oak Ridge, TN.

**Acknowledgement:** The authors wish to thank Dr. Wolfgang Boehme, Dr. Thomas Reichert (IWM Freiburg) and Dr. Uwe Mayer (MPA Stuttgart) for providing experimental data and helpful discussions.